AIAA-2006-4821

An Inverted-Pendulum Thrust Stand for High-Power Electric Thrusters*

A. D. Kodys,† R. Murray,‡ L. Cassady,§ and E. Y. Choueiri¶
Electric Propulsion & Plasma Dynamics Laboratory
Mechanical & Aerospace Engineering Department
Princeton University, Princeton, NJ 08544
(Dated: June 26, 2006)

The inverted-pendulum method of thrust measurement for high-power electric thrusters is described analytically and experimentally. Two sources of uncertainty in the thrust measurements are investigated: those due to changes in the sensitivity of the inverted pendulum and those due to tare forces resulting from thermal stresses and electromagnetic forces acting on the flexural elements. An idealized analytical model shows that changes in sensitivity occur due to changes in the mass loading of the inverted pendulum and the temperature of the flexure elements. The sensitivity can be increased only at the expense of more stringent requirements on mass loading and thermal control. The results of the model are validated with measurements made using a carefully calibrated inverted pendulum thrust stand having several advantageous design features including gallium pots for current conduction, an optical two-axis displacement sensor, and careful consideration of flexure shape and cooling requirements. The sensitivity is shown to be constant over a wide range of operating conditions. Measurements show that thermal drifts of the stand are linear on the time scale of the thrust measurements and are less than 0.6% of the expected thrust. The thrust stand operation was demonstrated during experiments with a 30-kW lithium-fed applied-field magnetoplasmadynamic thruster. Under nominal conditions (400 A, 0.1 T, 17.5 mg/s) the thermal and electromagnetic tare forces were measured at less than 9% of the thrust and the total thrust uncertainty at $\leq 10\%$ of the thrust.

I. INTRODUCTION

The direct measurement of the thrust of high-power electric thrusters such as the magnetoplasmadynamic thruster (MPDT)[1–3] is fraught with a number of challenging problems. Low thrust to mass ratios (<25 mN/kg), large thermal loads and cooling requirements, high, and often noisy, arc currents $\mathcal{O}$(100-10000 A) and strong applied magnetic fields (0.01-0.3 T) produce an environment which is hostile to thrust measurements. In one of the most promising MPDT variants, the lithium Lorentz Force Accelerator (Li-LFA)[3, 4], lithium propellant introduces additional and unique challenges. Thermal management, environmental (safety) constraints, materials compatibility, and more complex propellant feeding and metering systems increase the difficulty of obtaining thrust measurements.

One of the most successful methods of thrust measurement for high-power steady-state MPDTs is the inverted pendulum method first employed by Haag [5]. The inverted pendulum (IP), shown schematically in Fig. 1, consists of a platform holding the thruster, mounted on a support beam that is connected to the base by a flexural pivot, which allows the system to oscillate about the vertical position (an actual design is described in Section IV). The major benefit of the inverted design over the traditional hanging pendulum is that the mass of the system acts to augment the displacement rather than contribute to the restoring force. As we will show, this makes the sensitivity of the inverted pendulum more tunable and, in most cases, greater than a comparable hanging pendulum. Experience with the IP thrust stand design at Princeton University over the past several years has shown that the benefits of the IP design over the hanging pendulum are limited by thermal effects [6, 7]. Extensive experimental and anayltical studies of the behavior of the IP system have led to improvements in the understanding of the IP behavior and to modifications to the original design, as well as insight into optimal design practices, calibration and measurement procedures. In this paper we present the insight gained from these analytical and experimental efforts and demonstrate the measurement of thrust using a 30-kW lithium-fed MPDT.

In section II, we present an analytical model of the inverted pendulum and demonstrate how the sensitivity of the system can be adjusted through the proper choice of stiffness, flexure length, and load mass. In section III, we use these results to estimate the un-

---

*Presented at the 42^{nd} AIAA/ASME/SAE/ASEE Joint Propulsion Conference.
†Graduate Student, NASA Graduate Student Research Program, Princeton Plasma Science and Technology Program
‡Post-Doctoral Fellow at EPPDyL
§Graduate Student, National Science and Engineering Graduate Fellow
¶Chief Scientist, EPPDyL; Associate Professor, Applied Physics Group; Associate Fellow, AIAA; e-mail: choueiri@princeton.edu

certainty in the thrust measurement due to variations in mass on the stand and/or thermal variations in the flexures. The Princeton Inverted Pendulum Thrust Stand (PIPTS) is described in detail in Sec. IV. The results of the analytical model are verified by calibration of the PIPST. Calibration also quantifies the tare forces to improve measurement accuracy. The calibration procedure and results are presented in Sec. V. Finally, we demonstrate the operation of the PIPTS with thrust measurements taken during the operation of a 30-kW lithium-fed MPDT in Sec. VI.

II. AN IDEALIZED ANALYTICAL MODEL OF THE INVERTED PENDULUM

The general formulation of the equation of motion for any ideal pendulum can be obtained by equating the time-derivative of the angular momentum about the pivot point to the sum of the torques acting about the same point. Assuming motion in a single direction (θ) we can write

$$I\ddot{\theta} = L\sum F, \tag{1}$$

where I is the mass moment of inertia about the pivot axis, θ is the position angle, and L is the height of the center-of-mass above the pivot point. The total force, F, is the sum of the restoring, damping, and external forces acting upon the system. In the ideal model, it is assumed that the force is applied at L. Referring to Fig. 1, for the case of the ideal inverted pendulum, we consider the following forces

- A restoring force will be present due to the stiffness, k, of the flexure material and is proportional to the displacement. This force will act to return the stand to its equilibrium position when perturbed by an external force

$$F_{\text{rest}} = -kz \approx -k(L\theta), \tag{2}$$

  where the final expression is valid in the small angle approximation; $\sin\theta \approx \theta \approx z/L$.

- In the inverted pendulum geometry, gravity is not a restoring force but acts to increase the displacement from the equilibrium (vertical) position. The component in the direction of the torque is

$$F_{\text{grav}} = Mg\sin\theta \approx Mg\theta, \tag{3}$$

  where M is the total mass supported by the flexures, g is the acceleration due to gravity, and, again, we have made the small angle assumption.

- A damping force, due to friction in the system, is also present in the usual form:

$$F_{\text{damp}} = \nu\dot{z} = \nu(L\dot{\theta}), \tag{4}$$

  where ν is the damping coefficient.

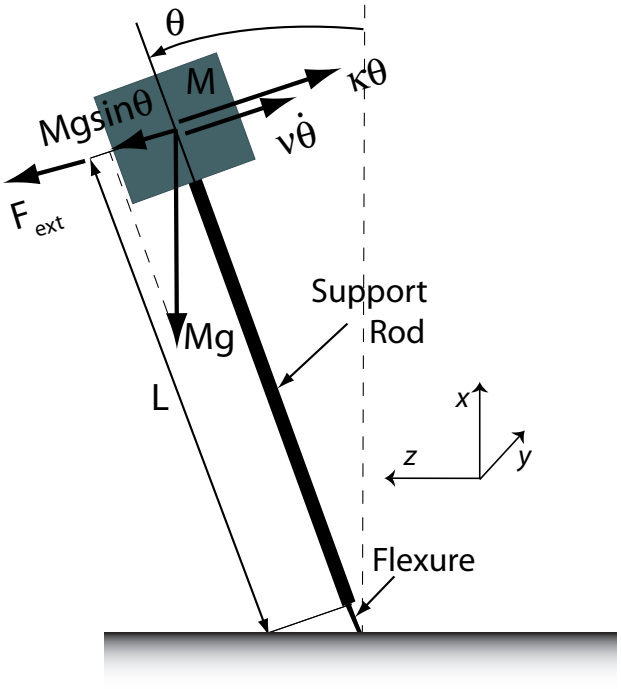

FIG. 1: Schematic of an ideal inverted pendulum showing dimensions and forces acting on the flexural element.

- Finally, an external force of the form $F_{\text{ext}}(t)$ acts on the system. In our case, the force will be a simple step function (steady-state thrust, T) which we take to act on the equilibrium system at $t = 0$

$$F_{\text{ext}}(t) = \begin{cases} 0, t < 0 \\ T, t > 0 \end{cases}. \tag{5}$$

  Additional tare forces due to thermal stresses and/or electromagnetic interactions may also be present in the actual system. These forces are determined by calibration and subtracted from the measured force to determine the true thrust force. The calibration method will be described in Section V

Inserting these forces into Eq. 1, and arranging it in the usual form, we get the equation of motion for an ideal inverted pendulum

$$\ddot{\theta} + 2\beta\dot{\theta} + \omega_o^2\theta = a, \tag{6}$$

where

$$\beta \equiv \frac{\nu L^2}{2I}, \tag{7}$$

$$\omega_o \equiv \sqrt{\frac{Lg}{I}\,(M_{\text{eff}} - M)}, \tag{8}$$

$$M_{\text{eff}} \equiv \frac{kL}{g}, \tag{9}$$

and

$$a \equiv \frac{LF(t)}{I}. \tag{10}$$

We see from the above expressions that the net restoring torque acting on the inverted pendulum is the difference between the torque due to the stiffness of the flexures and the gravitational torque. Thus, we expect the quantity $(M_{\text{eff}} - M)$ to be an important design parameter in optimizing the sensitivity of the stand. The damping coefficient $(\beta = \nu L^2/2I)$ will determine how quickly the system reaches its equilibrium position after a disturbance.

Assuming that at $t < 0$, when no external force is acting, the stand is at rest and that its equilibrium position is vertical $(\theta = 0)$, we can write the initial conditions

$$\theta(t = 0) = 0 \tag{11}$$

$$\dot{\theta}(t = 0) = 0, \tag{12}$$

and obtain the well-known solution to the damped oscillator equation:

$$\theta(t) = \frac{a}{\omega_o^2}\left[1 - e^{-\beta t}\left(\cos\omega_1 t - \frac{\beta}{\omega_1}\sin\omega_1 t\right)\right], \tag{13}$$

where ω_1 is the "frequency" of the damped oscillator and is defined by

$$\omega_1^2 \equiv \omega_o^2 - \beta^2. \tag{14}$$

For steady-state thrust measurements we are interested in the final displacement of the stand when a steady-state force is applied. Solving Equation 13 for $t \to \infty$, we have

$$\theta(t \to \infty) = \frac{a}{\omega_o^2} = \frac{T}{g(M_{\text{eff}} - M)}, \tag{15}$$

where

$$M_{\text{eff}} = \frac{kL}{g}$$

. If we can accurately measure the displacement angle of the IP stand and determine the design parameters k, M, and L by measurement or calibration, the applied force can be calculated directly from

$$T = g(M_{\text{eff}} - M)\theta. \tag{16}$$

Rearranging 16, we obtain an expression for the sensitivity of the inverted pendulum:

$$S \equiv \frac{\theta}{T} = \frac{1}{(kL - gM)} = \frac{1}{g(M_{\text{eff}} - M)} \quad [\text{rad/N}]. \tag{17}$$

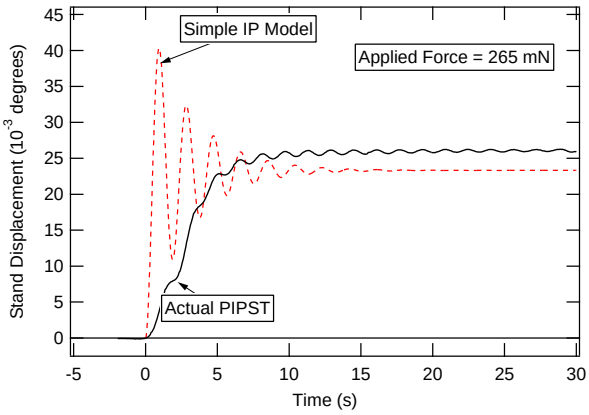

FIG. 2: A comparison of the response of the idealized IP model with the actual response of the PIPTS. The idealized model is shown to capture the frequency of the PIPTS well, but not the damping.

It should be noted that for the ideal case, the final displacement of the stand is independent of the mass moment of inertia of the system. If desired, I can be calculated from the empirically determined natural frequency, ω_o and stiffness, k.

From the steady-state solution in Eq. 17, it is clear that the sensitivity of the ideal IP is a function of only the height of the center of mass above the flexures (L), the total mass supported by the flexures (M), and the stiffness of the flexure material (k). In theory, the sensitivity can now be calculated. In practice, however, only M can be easily measured; the accurate determination of k and L are difficult (see additional discussion in Sec. III B). The uncertainty in the sensitivity can be reduced if careful calibration is used to determine the displacement angle (θ) for a known applied force. From such data experimental estimates of k or kL can be determined. The calibration procedure is discussed in Section V. For now, we simply state the result that the typical sensitivity of the Princeton Inverted Pendulum Thrust Stand (PIPTS) for small deflections from the vertical axis $(\theta = 0)$ is $S = 0.088 \pm 0.006$ deg/N (refer to Fig. 2). Assuming a point mass of 100 kg located at $x = L$ so that $I \approx ML^2$ we can estimate typical values for k and M_{eff}:

$$k_{\text{PIPST}} = \frac{1}{LS_{\text{PIPST}}} + \frac{gM}{L} = 2794 \ \text{ N/m}, \tag{18}$$

$$M_{\text{eff}} = \frac{kL}{g} = 166 \text{ kg}. \tag{19}$$

From the Idealized IP model, we predict the natural frequency of the stand to be approximately 0.54 Hz and the oscillations to be completely damped out within 20 seconds. Fig. 2 shows a comparison of the theoretical and experimental responses. Considering the simplicity of the idealized model, it does capture

the frequency of the oscillations fairly well (calculated: 0.54 Hz; measured: 0.62 Hz). The damping behavior is captured less well and this may be attributed to the finite time it takes for the calibration weights to be added to the stand: the initial larger amplitude oscillations (if they exist) are masked by the addition of the weights over the first five seconds. Moreover, the oscillations in the PIPTS take a much longer time to damp out than the model predicts. This may be attributed to the motion of the hanging calibration weights, which swing for several tens of seconds once they have been applied, and to facility vibrations which may excite the stand motion over a longer period.

From examination of Eq. 17 several design constraints on the inverted pendulum become immediately clear. First, the IP becomes unstable as $\bar{M} \equiv M_{\rm eff}/M \rightarrow 1$. For the case of an underdamped system, we therefore require

$$\bar{M} = \frac{kL}{gM} > 1 \tag{20}$$

for the design to be stable. This requirement sets the minimum value of kL for the flexures based on the mass of the thruster and subsystems supported by the stand.

Second, the greatest sensitivity will be obtained when the difference between the load and the effective mass is as small as possible. Based on these observations, it is tempting to design a stand with $\bar{M}$ as close to unity as possible. However this is not always optimum. Additional constraints on the sensitivity should be considered. These include

- The extent of the validity of the linear (small angle) approximation.
- The resolution and range of the position detector.
- The magnitude of noise (thermal, electrical, etc.) in the system.
- The expected magnitude of the applied force (T).
- The elastic limit of the flexures.

In addition to these constraints, we will see in Sec. III B that there is a penalty is to be paid for operating close to the unstable limit of the IP. The cost of high sensitivity to an applied force will be shown to be an increase in sensitivity to thermal changes in the flexure elements.

In Figure 3 we show how the sensitivity varies with the parameter $\bar{M}$ for the IP design. A typical operating point for the PIPTS is at $\bar{M} \approx 1.66$. As $\bar{M}$ becomes large, the sensitivity is a function of only the design parameters, and $S_{\rm min} \approx 1/(kL)$. This defines the minimum sensitivity for a given IP design. For a given IP design, the sensitivity can be tuned along this curve by adding or subtracting mass from the stand. The curve for the equivalent regular pendulum is plotted in the figure for reference. It is interesting to note (from the same plot) that the minimum sensitivity (0.035 deg/N) of the PIPST, which occurs at $\bar{M} \approx 2.66$, is about 60% that of an equivalent regular pendulum (0.058 deg/N) with the same load ($M = 100$ kg).

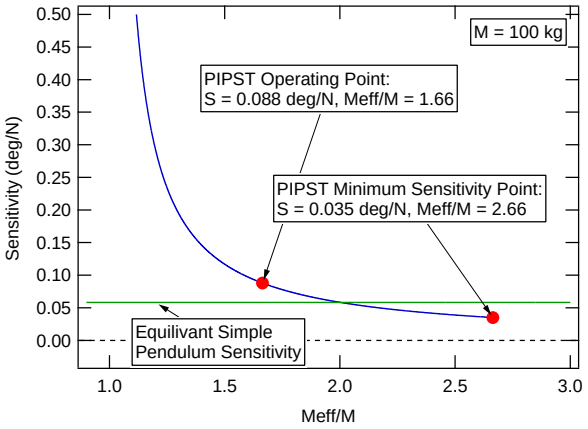

FIG. 3: Sensitivity versus $\bar{M}$ for the ideal IP thrust stand. The operating point and minimum sensitivity point for the PIPTS design are shown. The sensitivity of the IP can be tuned along this curve simply by adjusting the total mass load on the stand (for a fixed design; L, k). The sensitivity of an ideal regular (hanging) pendulum with an equivalent mass load is plotted for comparison.

From Eq. 16 we see that uncertainty in the thrust measurement can arise due to variations in the sensitivity of the stand during a thrust measurement or due to changes in θ from forces other than thrust. Changes in the sensitivity may occur due to changes in the stiffness of the flexures or in the mass they support. The uncertainty in the thrust measurements due to changes in sensitivity are examined next in terms of the idealized model. Additional forces may be present due to thermal stresses in the flexures or electromagnetic interactions between the changing currents and/or the applied magnetic field and the flexures. These tare forces are determined through careful calibration of the thrust stand which will be described in Sec. V

III. MEASUREMENT UNCERTAINTY DUE TO CHANGES IN SENSITIVITY

Previous experience with the inverted pendulum thrust stand design has shown that thermal variations in the flexure elements during thrust measurements may occur due to radiation and conduction from the thruster. Small changes in the mass on the stand may also occur due the the expulsion of propellant in the case where the propellant reservoir is also located on the stand (as is the case of our lithium MPDT set-up).

In this section we investigate the magnitude of these changes and predict their contribution to the uncertainty of the thrust measurement.

In the following analysis, we assume that the only applied force is thrust. We also assume that the change in angle of the stand ($\Delta\theta$) can be measured perfectly (i.e. with no error). Under these additional constraints, and those inherent in the idealized model, we see that thrust is a function only of the total mass supported by the flexures (M), and the effective stiffness of the flexures (kL). It is important to note here that we measure thrust with the inverted pendulum thrust stand by establishing steady-state operation of the thruster and then turning the thruster off and measuring the displacement of the inverted pendulum. We require up to two minutes of data before and after the termination of the thrust to accurately establish the position of the thrust stand. Variations in M, L, or k, on the time scale of the thrust measurement will introduce uncertainty into the measurement by changing the effective sensitivity $S = \Delta\theta/T$ of the stand. Since it is the *difference* between the effective mass(kL/g) and the mass (M) which sets the sensitivity, we expect that the uncertainty will be a function of the design parameter $M(\bar{M}-1)$ where $\bar{M} \equiv M_{\rm eff}/M$.

We first examine the most general case and find an expression for the uncertainty as a function of changes in the value $(M_{\rm eff}-M)$. Then, in the remainder of this section, we examine the effect of each of the individual design parameters on the uncertainty and show how the uncertainty per percent change in these parameters depends on the design sensitivity (or $\bar{M}$). Finally, we estimate the typical expected variation in M, L, and k over the course of a thrust measurement and use this information along with estimates of the thrust uncertainty due to changes in these parameters to predict the minimum uncertainty for a given inverted pendulum design.

In the most general sense, we can express the uncertainty in the thrust measurement as the fractional change in sensitivity ($\Delta S/S$) on the time scale that the measurement is made:

$$U_T \approx \frac{\Delta S}{S} = \frac{1}{gS}\left[\frac{1}{(M_{\rm eff}-M)_{\rm pre}} - \frac{1}{(M_{\rm eff}-M)_{\rm post}}\right]. \tag{21}$$

Defining the fractional change in the quantity $\delta \equiv (M_{\rm eff}-M)$ as

$$\frac{\Delta\delta}{\delta} \equiv \frac{(M_{\rm eff}-M)_{\rm pre} - (M_{\rm eff}-M)_{\rm post}}{(M_{\rm eff}-M)_{\rm pre}}, \tag{22}$$

we can re-express the uncertainty in terms of $\Delta\delta/\delta$:

$$U_T \approx \frac{\Delta S}{S} = \frac{1}{gSM(\bar{M}-1)}\left[\frac{\Delta\delta/\delta}{\Delta\delta/\delta - 1}\right] = \frac{\Delta\delta/\delta}{\Delta\delta/\delta - 1}, \tag{23}$$

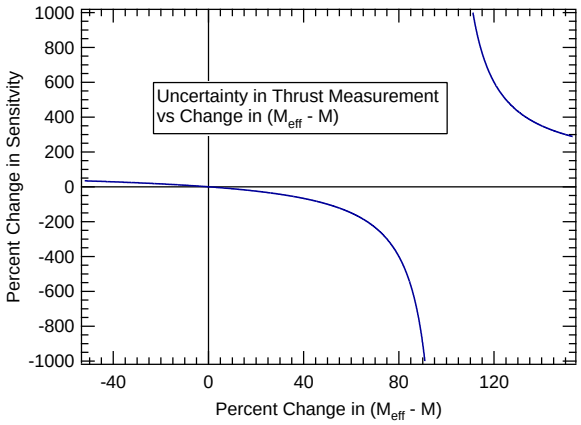

FIG. 4: Predicted percent change in sensitivity (thrust uncertainty) versus percent change in $(M_{\rm eff}-M)$. The sensitivity of the ideal IP design to changes in $(M_{\rm eff}-M)$ can be seen to increase dramatically in the vicinity of the point of instability (100% change in $(M_{\rm eff}-M)$).

where $\bar{M} \equiv M_{\rm eff}/M$ and

$$S = \frac{1}{gM(\bar{M}-1)}$$

Plotting the result for a range of $\Delta(M_{\rm eff}-M)$ values, we see in Fig. 4 that the uncertainty in the stand sensitivity (i.e. the minimum uncertainty in the thrust measurement) increases dramatically as the value of $(M_{\rm eff}-M)$ approaches zero (or, equivalently, $\Delta\delta/\delta$ approaches 100%). In Fig. 5 we zoom in on the range of reasonable thrust uncertainties ($U_T = \pm 5\%$) and examine how the uncertainty depends on $\Delta\delta/\delta$. In this range, the behavior of the curve is approximately linear. We see from this plot that if the uncertainty in the thrust measurement is required to be $\leq 2\%$, only about a $\pm 2\%$ change in the value $(M_{\rm eff}-M)$ can be tolerated. This relationship is approximately one to one for small uncertainties. This result was expected and gives us a feel for the overall trend, but we are more concerned with what happens to the uncertainty for small changes in the parameters we directly control (M, L, and k). Next, we examine the specific causes of variations in $(M_{\rm eff}-M)$ and estimate the effect that they each will have on $(M_{\rm eff}-M)$ and $\Delta S/S$. We start with changes in the total mass (M).

A. Thrust Uncertainty due to Changes in Total Mass

We first express $\Delta\delta/\delta$ in terms of the fractional (or percent) change in mass ($\Delta M/M$):

$$\frac{\Delta\delta}{\delta} = \frac{-\Delta M}{(M_{\rm eff}-M)} = \frac{1}{1-\bar{M}}\left(\frac{\Delta M}{M}\right), \tag{24}$$

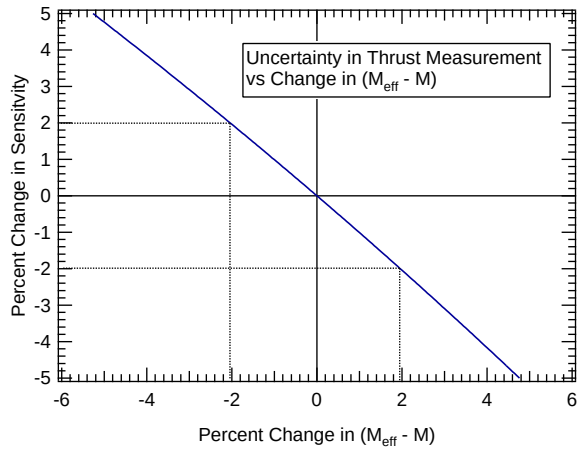

FIG. 5: A detail of Fig. 4 showing the percent change in sensitivity versus the percent change in $(M_{\text{eff}} - M)$. The percent change in sensitivity for a given change in $(M_{\text{eff}} - M)$ is seen to be approximately linear for small changes and to be approximately one to one.

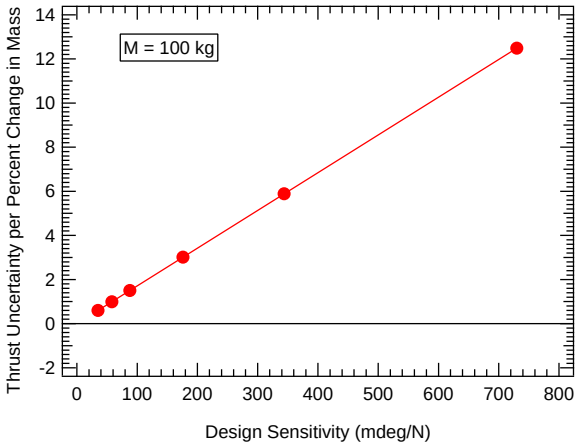

FIG. 6: Plot of equation 25: Thrust uncertainty per percent change in total mass vs design sensitivity. It is assumed that M_{eff} is constant and that $M = 100$ kg.

where $\Delta M \equiv M_{\text{pre}} - M_{\text{post}}$ and $M = M_{\text{pre}}$. The relationship between the percent change in $(M_{\text{eff}} - M)$ and the percentage change in M (assuming that M_{eff} is a constant) is therefore linear with a negative slope ($\bar{M}$ is always > 1) and is a function of the design parameter $\bar{M}$. We therefore expect that the relationship between the thrust uncertainty and the total mass will be a function of sensitivity. We make the results clearer and easier to use by plotting derivative of U_T with respect to the percent change in mass. For a constant M_{eff}, and in the limit of small changes in $\Delta M/M$, we have

$$\frac{\partial U_t}{\partial(\frac{\Delta M}{M})} \approx (gM)S, \tag{25}$$

which shows that the rate of change of the uncertainty with respect to $\Delta M/M$ (i.e the uncertainty per percent change in M) is a function of only the design sensitivity and the initial mass. Rearranging the above expression and expressing sensitivity in units of mdeg/N:

$$\Delta U_T \approx \frac{\pi g M S}{1.8 \times 10^5} \left[\Delta\left(\frac{\Delta M}{M}\right)\right]. \tag{26}$$

We can calculate the best uncertainty we can expect for a given sensitivity and variation in mass *or* we can determine what the maximum sensitivity can be for an expected change in mass and a given uncertainty requirement. We plot this result for a range of sensitivities ($M = 100$ kg) in Fig. 6. From this plot we see that if we increase the sensitivity of the stand from 88 mdeg/N to 176 mdeg/N (a factor of 2 increase) then the uncertainty would increase from 1.5% to 3% per percent change in mass. If we require the uncertainty to remain less than ±2%, we have tightened the requirements on the variation in M from $\leq 1.3\%$ at 88 mdeg/N to $\leq 0.67\%$ at 176 mdeg/N.

1. *Estimated Variation in Total Mass*

The only expected source of significant changes in mass during thruster operation is the loss of mass due to propellant feeding. In the case of our lithium-fed thruster, the lithium propellant is stored on the thrust stand and fed to the thruster using a mechanical piston (see [8] for details). The total mass on the stand is estimated to be approximately 100 kg for the 30 kW AF-MPDT. A conservative estimate for the mass flow rate of lithium through the thruster is 50 mg/s. The mass flow rate is constant during the thrust measurement. Since a meaningful thruster measurement is taken only when the stand has reached a thermal steady-state, it typically takes four minutes from start-up for a single thrust measurement. During that time 12 grams of lithium will be removed from the stand. The percent change in total mass on the stand is then

$$\frac{\Delta M}{M} = \frac{0.012}{100} = 0.012\%. \tag{27}$$

From Eq. 26 we can now estimate the uncertainty in thrust measurements due to a likely change in mass. We see that for the current stand design ($S = 88$ mdeg/N), the uncertainty due to lithium feeding causing a change in M will be $< 0.02\%$. Doubling the sensitivity of the stand, with the change in mass held constant, will double the thrust uncertainty. If the entire load of lithium on the thrust stand (300 g) was expelled at once while thrust was being measured, the contribution to the uncertainty would be less than 0.5% at 88 mdeg/N, and the stand sensitivity could be increased more than four times to 389 mdeg/N before the uncertainty would increase above 2%. From

this analysis, it appears that, for typical operation, the small changes in mass that we expect during thrust measurement will not contribute significantly to the thrust uncertainty. At 88 mdeg/N, we would require a change in mass of greater than 1.3% before the uncertainty would increase above 2%.

B. Thrust Uncertainty due to Changes in M_{eff}

From a practical standpoint, we expect changes in the stiffness of the flexures, k, on the time scale of the thrust measurement to be one of the major sources of error. We can estimate the effect of changes in flexure stiffness by examining the behavior of M_{eff}. Following the above procedure, we can write

$$\frac{\Delta\delta}{\delta} = \frac{1}{1-\frac{1}{M}}\left(\frac{\Delta M_{\text{eff}}}{M_{\text{eff}}}\right) \tag{28}$$

Since $M_{\text{eff}} = kL/g$, the fractional (or percent) change in M_{eff} is equivalent to the fractional change in k, L, or the product kL with the other terms held constant. So we can write

$$\frac{\Delta M_{\text{eff}}}{M_{\text{eff}}} = \frac{\Delta(kL)}{kL} = \left.\frac{\Delta k}{k}\right|_{L=\text{constant}}. \tag{29}$$

By substituting this expression into the expression for the fractional change in sensitivity (Eq. 23) we obtain the thrust uncertainty as a function of the fractional change in M_{eff}. To find the relationship between the uncertainty in thrust per percent change in M_{eff} and the IP sensitivity, we again take the derivative of U_T ,this time with respect to $\Delta M_{\text{eff}}/M_{\text{eff}}$. For a constant M, and in the limit of small changes in $\Delta M_{\text{eff}}/M_{\text{eff}}$, we have

$$\frac{\partial U_T}{\partial(\Delta M_{\text{eff}}/M_{\text{eff}})} \approx -1 - (gM)S. \tag{30}$$

This is plotted in Fig. 7 along with curve from Fig. 6 for comparison. We see that while the slopes of the two curves are of the same magnitude, they are in opposite directions, and the absolute magnitude of the uncertainty per percentage change is larger (by +1) for changes in the effective mass. For instance, while a 1% increase in the total mass on the stand will result in an 1.5% percent change in the sensitivity (at $S = 88$ mdeg/N), the same percentage increase in the effective mass will result in a -2.5% change in sensitivity.

Rearranging Eq. 30 and expressing sensitivity in units of mdeg/N, we have

$$\Delta U_T \approx -1 - \frac{\pi g M S}{1.8\times10^5}\left[\Delta\left(\frac{\Delta M_{\text{eff}}}{M_{\text{eff}}}\right)\right]. \tag{31}$$

This implies that, for our design point of 88 mdeg/N,

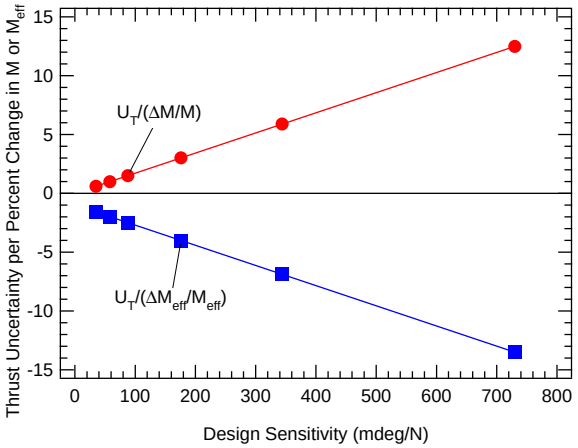

FIG. 7: Plot of equation 30. Thrust uncertainty per percent change in total mass vs design densitivity. It is assumed that M_{eff} is constant and that $M = 100$ kg. The curve from Fig. 6 is shown for comparison.

if the thrust uncertainty is to be kept below ±2%, the variation in M_{eff} during the measurement must not exceed ±0.80%. If we are able to estimate the expected variation in M_{eff} during the measurement and know it to be closer to ±1.5%, we can estimate the maximum sensitivity we can design for and still maintain $U_T \leq 2\%$. Solving Eq. 31 with $U_T = 2\%$ and $\Delta M_{\text{eff}}/M_{\text{eff}} = 1.5\%$, we find that the sensitivity cannot be greater than about 29 mdeg/N while still meeting these requirements. This is well below the sensitivity of a similar hanging pendulum stand (58 mdeg/N) and demonstrates the importance of controlling the flexure properties for the implementation of a good IP design. In order to design a IP thrust stand with equal to or greater sensitivity then an equivalent hanging pendulum and a minimum thrust uncertainty of ±2%, the idealized analaytical model prescribes that the changes in the effective mass must be kept to less than ±1% during the measurement.

We have shown that changes in M_{eff} on the time scale of the thrust measurements can result in unacceptably large uncertainties or undesirably low stand sensitivities. Care must be taken then to ensure that all sources of variation are accounted for. We have mentioned previously that the largest source of variation in M_{eff} are likely to be due to variations in k due to changes in the temperature of the flexural elements. How strongly k is a function of temperature will determine how stringent the constraints on $\Delta k/k$ are. Next we develop an analytical expression for k and examine how it will respond to changes in temperature.

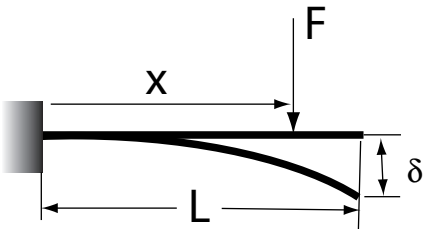

FIG. 8: Cantilever beam deflecting under load F applied at the tip for estimating k.

1. Estimating The Flexure Stiffness, k

The effective spring constant of each flexure can be estimated by assuming a long, slender beam and employing the Euler-Bernoulli beam equation. Considering the long slender cantilever beam in Fig. 8 with a length L. A force F is applied at the tip of the beam such that the deflection at that location is δ. From Hooke's Law we have

$$k = \frac{F}{\delta}. \tag{32}$$

The deflection distance, δ, depends on the material properties and dimensions of the beam according to the Euler-Bernoulli beam equation:

$$\frac{d^2y}{dx^2} = \frac{M(x)}{EI}, \tag{33}$$

where $M(x) = F(L - x)$ is the sum of the moments about x, E is the Young's Modulus of the beam material, and I is the area moment of inertia of the beam. Differentiating twice:

$$y(x) = \frac{FLx^2}{2EI} - \frac{Fx^3}{6EI} + C_1x + C_2, \tag{34}$$

and applying the initial conditions:

$$y(0) = 0 \tag{35}$$

$$\frac{dy}{dx}(0) = 0, \tag{36}$$

we find

$$y(x) = \frac{FL}{6EI}\left(3Lx^2 - x^3\right). \tag{37}$$

To find the deflection at the tip we solve for $y(L)$ and then substitute the result into Eq. 32 :

$$\delta = y(L) = \frac{Fl^3}{3EI}, \tag{38}$$

$$k = \frac{3EI}{L^3}. \tag{39}$$

Using the typical PIPST values; $L = 0.58$ m, $E_{\mathrm{Cu}} \approx 117$ GPa, and

$$I = \frac{\pi}{64}(D^4 - d^4) = 3.2 \times 10^{-10} \quad \mathrm{m}^4,$$

where $D = 9.52$ mm is the flexure outer diameter, and $d = 6.35$ mm is the flexure inner diameter, the estimated value of k for a single flexure is

$$k = 571 \quad \mathrm{N/m}. \tag{40}$$

The total effective k_{eff} of the system can be found by adding the individual k's:

$$F = k_{\mathrm{eff}}z = k_1z + k_2z + k_3z...k_nz, \tag{41}$$

with

$$k_{\mathrm{eff}} = k_1 + k_2 + k_3...k_n \approx nk, \tag{42}$$

where we have assumed that k is the same for all n flexures:

$$k_{\mathrm{eff}} \approx nk. \tag{43}$$

For the PIPST, where $k = 571$ N/m and $n = 6$, we have $k_{\mathrm{eff}} \approx 3430$ N/m, which is about 25% higher than the value found empirically from the measured sensitivity of the stand (2750 N/m).

From Eq. 39 we see that changes in the stiffness are likely to rise due to changes in Young's Modulus or the dimensions (D, d, and/or L) of the flexures. The most obvious cause for such changes is a temperature change in the flexures due to thermal conduction from the hot thruster, radiation from the plume, current conduction along the flexure, or a change in temperature of the coolant flowing through the flexures. We first estimate the expected change in E with temperature and, in the following paragraphs, tackle the problem of variations in flexure diameter and length.

2. Uncertainty Versus Change in Flexure Temperature: Variations in E

The variation in Young's Modulus of the copper flexures with temperature will be on the order of 0.04 %/ K. For now, we will assume that this change is large compared to any changes in the dimensions of the flexures due to temperature. Therefore, we can re-express $\Delta k/k$ in terms of a temperature change(ΔT) in the flexures:

$$\frac{\Delta k}{k} \approx \frac{\Delta E}{E} \approx 4 \times 10^{-4}\Delta T. \tag{44}$$

In figure 9 we plot the change in stand sensitivity versus the change in the temperature of the flexures. We assume that the only effect of that temperature change is to change Young's Modulus of copper by 0.04%/K.

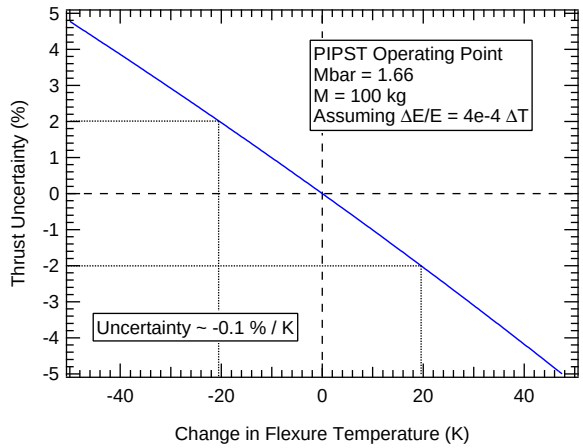

FIG. 9: Change in PIPTS sensitivity versus the change in flexure temperature under the assumption of constant flexure dimensions and a change in E of 0.04%/K. It appears that temperature changes of ± 20 K should be tolerable with a less than 2% change in stand sensitivity.

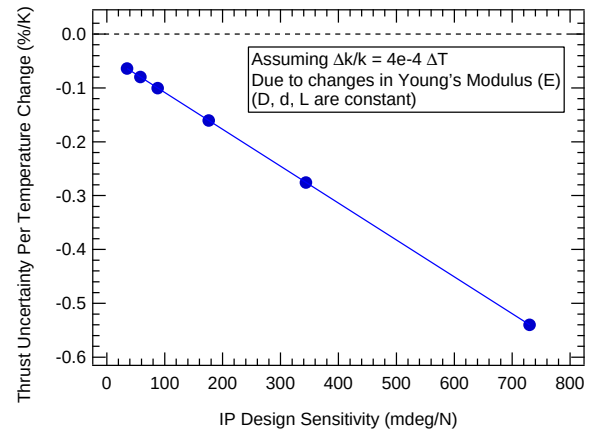

FIG. 10: Percent uncertainty in thrust measurement per degree Kelvin change in flexure temperature. Change in flexure stiffness is assumed to be due only to changes in the Young's modulus of the copper flexures with temperature. $\Delta E/E \approx 4\times10^{-4}\Delta T$ with T in degrees Kelvin is assumed.

To maintain the sensitivity error at less than 2%, under these assumptions, we should be able to tolerate a change in flexure temperature of no more than ± 20 K.

In Fig. 10, we plot the thrust uncertainty per degree Kelvin temperature change in the flexures versus stand sensitivity by replacing $\Delta M_{\rm eff}/M_{\rm eff}$ in Eq. 31 with $0.04\Delta T$. From the plot, we expect a 0.1%/K uncertainty for our design point of 88 mdeg/N. The percent uncertainty per degree Kelvin increases linearly as the sensitivity of the stand increases. Approximately doubling the sensitivity to 176 mdeg/N would result in a thrust uncertainty of 0.16 %/K and requires approximately twice as good thermal control ($\Delta T \leq 12$ K) to maintain the acceptable uncertainty ($\pm 2\%$).

3. *Uncertainty Versus Change in Flexure Temperature: Variations in Flexure Shape*

For the hollow tube geometry of our stand's flexures, we can write I, the area moment of inertia, as

$$I = \frac{\pi}{64}\left(D^4 - d^4\right), \tag{45}$$

where D is the outer diameter of the flexure and d is the inner diameter which implies, through Eq. 39, that the stiffness of the flexure element is dependent on its dimensions D, d, and L (for a constant E).

Since the copper tubes are rigidly attached to the tank at their base and to the thruster plate at their top, we will tak, as a first approximation, the length, L, of the flexures to be fixed. Although the flexures could expand along their length moving the thruster plate by ΔL, the weight of the thruster (100 kg) should be sufficient to prevent any axial expansion. Thermal stresses will develop due to this constraint, but the resulting tare forces are beyond the scope of this model and are addressed by careful calibration of the stand. In the radial direction, however, we assume the flexures are free to expand without bound. Under these assumptions, we can express the change in flexure stiffness (i.e the change in $\Delta M_{\rm eff}/M_{\rm eff}$, see Eq. 29) in terms of changes in the diameter of the flexures as

$$\frac{\Delta M_{\rm eff}}{M_{\rm eff}} = \frac{\Delta k}{k} = \frac{\left[(D+\delta_D)^4 - (d+\delta_d)^4\right] - (D^4 - d^4)}{(D^4 - d^4)}. \tag{46}$$

In order to estimate the change in stiffness, we need to find expressions for δ_D and δ_d, which represent the changes in the diameters D and d. If thermal expansion is unrestrained, we expect that all dimensions will expand equally and that the expansion will be proportional to the temperature change according to the relation

$$\epsilon = \frac{\partial \delta_r}{\partial r} = \alpha \Delta T, \tag{47}$$

where the r subscript denotes a radial expansion. Solving for δ_r at D and d, we get

$$\delta_D = \alpha \Delta T D \qquad \delta_d = \alpha \Delta T d, \tag{48}$$

and substituting this expression into Eq. 49, we find after some simplification

$$\frac{\Delta k}{k} = 4\alpha\Delta T + 6\alpha^2\Delta T^2 + 4\alpha^3\Delta T^3 + \alpha^4\Delta T^4 \approx 4\alpha\Delta T. \tag{49}$$

This is the desired expression for $\Delta k/k$ in terms of changes in temperature where the last approximation is valid for $\alpha = \mathcal{O}(10^{-5})$ K^{-1} and $\Delta T = \mathcal{O}(1-10)$ K. We note that the percentage change in k is independent of the dimensions of the flexures.

Since α is small (17×10^{-4} % K^{-1} for copper) and we expect changes in temperature of only a couple of

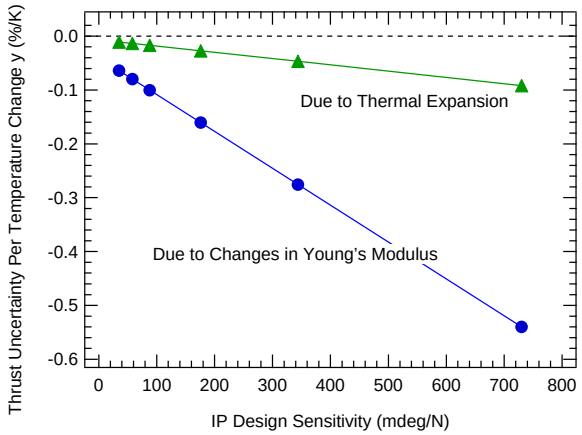

FIG. 11: Percent uncertainty in thrust measurement per degree Kelvin change in flexure temperature. Changes in flexure stiffness are due to predicted variations in the Young's modulus or the diameter of the copper flexures with temperature. $\Delta E/E \approx 4 \times 10^{-4}\Delta T$ and $\Delta k/k \approx 6.8 \times 10^{-6}\Delta T$with T in degrees Kelvin

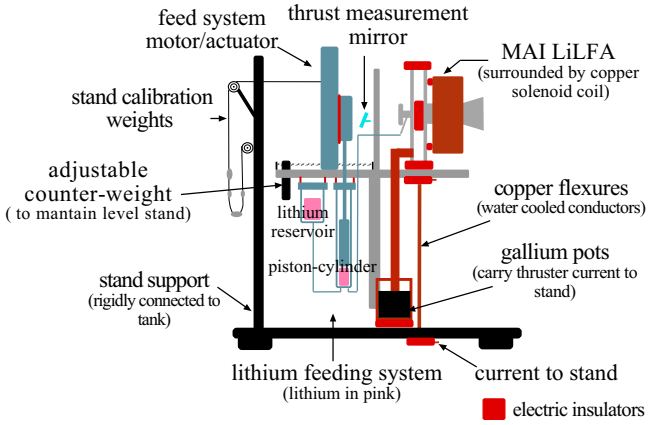

FIG. 12: A schematic (not to scale) of the Princeton inverted pendulum thrust stand (PIPTS). The flexure elements are six 1/4-inch copper tubes, 35.6 cm in length. The PIPTS is shown with the 30-kW AF-MPDT and its subsystems in place.

degrees Kelvin on the time scale of the measurements, we can easily see that the effect of thermal expansion on the IP sensitivity will be small. Substituting Eq. 49 into Eq. 31, we find that the effect is approximately an order of magnitude smaller than that associated with changes in E. The two results are plotted together for completeness in Fig. 11. Based on this analysis, we conclude that the inverted pendulum stand sensitivity is effectively unaffected by changes in the flexures' temperature.

IV. DESCRIPTION OF THE PRINCETON INVERTED PENDULUM THRUST STAND

The PIPTS system is shown schematically in Fig. 12. The main elements of the system are the flexures and thruster support plate, the thermal control system, the liquid gallium pots for current conduction to the thruster, the *in situ* leveling and calibration systems, and the laser-based, non-contact displacement measurement system (not shown). While details of the system were discussed in Refs. [6, 7], we give here a description of the key features of the design:

- The flexures are 1/4-inch copper (alloy 122) straight tubing (3/8-inch (9.53 mm) outer diameter) with a 0.065-inch (1.65 mm) wall thickness and 35.6 cm in length.

- The conduction of current to the thrust stand is done through gallium pots at the base of the stand. It has been demonstrated by us [7] and by others [9–12] that liquid metal conductors reduce tare forces due to thermal stresses and electromagnetic interactions between conductors. Gallium is non-toxic and has the largest liquid range of any element; melting at just above room temperature (29.8 $°C$) and remaining in the liquid state until 2403$°C$. In addition, its vapor pressure remains low even at elevated temperatures (10^{-8} Torr at 619 $°C$). Its electrical conductivity, 0.0678 $(\Omega\ \mathrm{cm})^{-1}$, is about 6 times that of mercury.

- The coolant for the thruster and subsystems flows through the copper tubes constituting the flexures. The coolant flow is supplied and removed from the stand through through 1/4-inch teflon tubes that are run parallel to the flexures. All the return coolant which experiences temperature variations over the course of a thrust measurement (thruster and stand cooling) is returned from the stand via two of these teflon tubes to minimize reactions on the stand due to changes in flexure temperature. This reduces the temperature variations of the flexures during the thrust measurements to acceptable levels.

V. PIPTS CALIBRATION

A series of calibration tests of the Princeton Inverted Pendulum Thrust Stand (PIPTS) were undertaken to characterize the stand behavior and to determine the following:

- Nominal thrust stand sensitivity.

- Magnitude of drifts in stand neutral position due to expected changes in center-of-mass and flexure temperature.

- Magnitude of tare forces.

The calibration tests were conducted with a 30-kW AF-MPD thruster from the Moscow Aviation Institute, its solenoid coil, and the lithium feed system placed on the stand in the operating configuration. Weight was added to the front of the stand to bring the neutral stand position as close as possible to vertical ($\theta = 0$) and to minimize twisting (i.e. to get the center of mass of the system as close to the thrust axis as possible). This was accomplished by trial and error due to the complexity of the mass distribution and the necessity of having the thruster and subsystem components in certain locations. A movable counterweight, which could be controlled remotely, allowed for fine adjustments of the stand tilt immediately prior to thruster operation.

The inverted-pendulum thrust stand determines thrust by measuring the change in position of the stand as the thruster is turned off. The applied force is determined from the measured change in angle of the inverted pendulum and the predetermined sensitivity of the stand. Sensitivity is determined from pre-experiment calibrations and from calibration checks immediately before and after the displacement measurement. Any tare (non-thrust) forces acting on the stand (determined by pre-firing calibration) are subtracted from the measured displacement and the result is the measured thrust.

The displacement of the thrust stand is measured as a voltage signal on a 2-D photo-diode array (PSD) (described in Ref. [6]). This can be converted into an actual displacement angle based on the geometry of the set-up and the size of the detector. For the discussion in this paper, however, this step is not required and we simply express $\Delta\theta$ in terms of mV and the sensitivity in terms of mV/mN.

In the most basic sense, the stand displacement is simply the difference between the voltage reading on the PSD while the thruster is operating at steady-state and the voltage reading after the thruster has been turned off. The situation is slightly more complicated in practice as we have:

- Noise in the voltage measurement. These are mostly due to electromagnetic interference from the experiment and mechanical vibrations of the stand. Although the signal to noise ratio is large, 10-100 individual points must be averaged to get an accurate measure of stand position.

- Drifts in stand position. These are linear and significant compared to thrust and can change in magnitude and direction as the thruster is turned on and off. These drift will be discussed in greater detail in the following section concerned with the sources of measurement error. Such drifts can introduce large uncertainties into the thrust measurement if simple averaging is used to determine stand position.

- The desire for a consistent (non-subjective) procedure for determining the magnitude of the displacement during calibrations of the stand and the actual thrust measurement.

To meet these requirements an algorithm was developed to determine the magnitude of the stand deflection during calibrations and thrust measurement. Since the inverted pendulum design exhibits a linear drift in position over many minutes, the basis of the algorithm is to fit a straight line to the stand position versus time data before and after the force is applied. The fit is done with 20 seconds of data (20-30 data points) to provide an adequate number of data points for the fit and to minimize the effect of noise in the voltage measurement. The displacement is determined by taking the difference between the values given by the two curve fits extrapolated back to the moment of the change in force.

A. Sensitivity

Calibration weights are added and removed with the stand under a variety of thermal, thruster current, and applied field configurations to verify that the sensitivity remains constant, as predicted by the idealized model. The sensitivity of the stand was found to be independent of the thermal state of the stand, the magnitude of the applied magnetic field (0-0.1 T), and the current to the thruster (0 -700 A) as long as the system was allowed to reach steady-state conditions. In Fig. 13 we summarize the sensitivity data obtained over the three runs of calibrations at different steady-state conditions. The average sensitivities for each run are 2.31 ± 0.07, 2.37 ± 0.1, and 2.07 ± 0.07 mV/mN respectively. Each data point is the average of 3-5 trials and the error bars are the 95% confidence uncertainty based on the standard deviation of the mean. The large error bars on a couple of the data points are because only a single trial was available at that operating condition. The good agreement with the other data points suggest a constant sensitivity. The average for the three calibration runs is 2.25 ± 0.14 mV/mN. The run-to-run variation in the sensitivity (6%) is about twice as large as the variation over a single run (3-4%) when operating over a range of steady-state conditions. This illustrates the importance of establishing the base-line sensitivity via stand calibration prior to each set of tests to minimize the uncertainity.

B. Neutral Position Drifts

There are two possible causes of drifts in the neutral position of the PIPTS during thrust measurement: changes in the center of the mass of the stand and slow changes in temperature of the stand components.

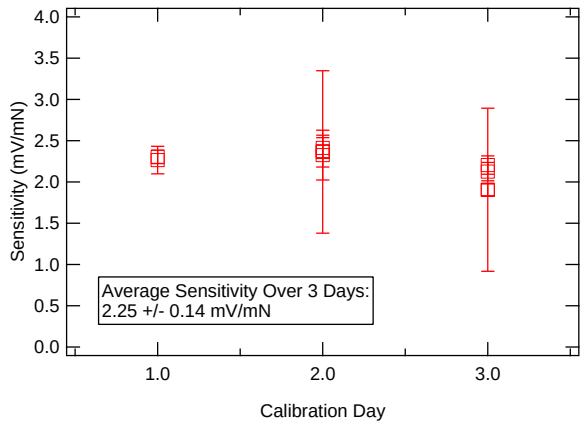

FIG. 13: The results of the sensitivity calibration of the PIPTS over three runs.

Changes in the center of mass of the stand arise due to the movement of the piston as it feeds the lithium propellant to the thruster (see [8] for a complete description of the lithium feed system). Thermal variations occur due to changes in the temperature of the coolant in the flexures, radiation from the thruster and plume, and/or conduction from the hot thruster components to the stand. It is important to perform calibrations to determine how changes in each of these parameters affect the thrust stand prior to taking thrust data. If the effects are small compared to the expected thrust, and are linear over several minutes, the data analysis procedure will reduce the error introduced by the neutral position drifts. If the effects are large or nonlinear, then the error may become unacceptably large despite the analysis techniques and design changes must be considered.

Thermal drift calibrations were conducted by monitoring the stand position as the flexure temperature was varied by changing the temperature of the coolant. The sensitivity was constant throughout the test and did not vary with the temperature of the flexures. By plotting the change in stand position vs the change in flexure temperature for several different steady-state temperatures we determined that the average neutral position drift due to thermal effect is -1.5 ± 0.7 mN/C at 95% confidence. From temperature data taken during thruster operation we see that the temperature change in the flexure coolant over the 2-4 minutes of the thrust measurement was never more than $1°C$. Therefore, the change in stand position due to thermal drifts will never be greater than 1.5 mN or 0.8% of the thrust. The calibration also showed that the thermal drift is linear over this time scale, and will easily be accounted for in the data analysis routine, thus reducing the error even further.

The placement of the lithium feed system on the thrust stand introduces additional complexities to the measurement of thrust. Vibrations induced by the stepper motor, thermal loads due to feed system heating and cooling, and the motion of the piston and lithium on the stand may cause changes in the sensitivity of the stand or drifts in the neutral position. Vibrational effects due to the operation of the feed system motor are negligible compared to the thrust (typically 200-700 mN). The effect of thermal loading was discussed in the previous paragraphs and is minimized by operating the feed system at a constant temperature during thrust measurement. In Sec II we showed that, in the idealized model, any change in sensitivity due to the reduction in mass on the stand due to the removal of lithium propellant will be small. The idealized model, however, does not account for changes in the center of mass on the stand due to the movement of the piston as it expels the lithium. Calibrations were conducted to determine the effect of lithium feeding (changes in the center of mass location on the stand) on the sensitivity and the neutral position of the stand. The tests were conducted with the PIPTS in the experimental configuration, except that the stand was cold. No thermal loads were placed on the stand and the temperature in the flexures remained constant at 18 $°C$ during the entire test in order that we could separate out the thermal and center-of-mass shift effects. The sensitivity of the stand was determined following the standard calibration procedure at a variety of mass flow rates and piston positions. The sensitivity was constant over the entire range and speed of piston motion with no apparent dependency on pistion location, or mass flow rate. The sensitivity of the PIPTS design therefore appears to be unaffected by the center-of-mass changes due to lithium feeding. However, there is a small linear drift in the stand neutral position due to the movement of the center of mass of the stand. Using the worst case scenario of a 200 mg/s mass flow rate (typical flow rates for this thruster are 5-20 mg/s), the neutral drift is estimated to be 0.00092 ± 0.0002 mN/s. Over the four minutes (maximum) required to reach a steady state and obtain a single thrust measurement, this translates to a drift in the PIPTS position of 0.22 ± 0.04 mN (at 95% uncertainty) or less than 0.1% of the expected thrust. The center-of-mass drift is linear during constant lithium feeding, and is nearly an order of magnitude smaller than the thermal drift. Since thrust measurements are taken during periods of constant lithium feeding, and the effect is small compared with thermal effects, the error due to lithium feeding is adequately accounted for in the data analysis routine and no further consideration is given to changes in the center-of-mass of the stand.

C. Measurement of Tare Forces

The thruster and its subsystems are brought as close as possible to operating conditions (including running

current through the shorted thruster), the sensitivity of the stand is established, and then the stand deflection is measured as the thruster current is turned off. Measurements were obtained over three runs of calibrations at several currents (500-700 A) and applied field strengths (0-0.1 T). No clear trend in the data with current or magnetic field was observed. Due to the small nature of the stand deflections related to changes in thruster current, a calibration weight (132.5 mN) was removed at the same time as the current was turned off. The known force due to the calibration weight was then subtracted from the total measured force. This procedure resulted in a larger total displacement of the stand and reduced the uncertainty in the measurement. The results of the tare force calibration are presented in Fig. 14. Each data point represents the average of 3-5 trials and the associated 95% uncertainty interval. No dependency on thruster current was found over this small current range. The correction to the measured thrust due to tare forces on the stand was calculated from the average of all the data taken over the three runs of calibration. The tare force correction is

$$F_{\text{tare}} = -21 \pm 6 \ \text{ mN}.$$

This force is negative on the transition to current off (i.e. as the thrust force is removed from the stand); therefore the tare force is seen to act in the same direction as the thrust force. The tare force must therefore be subtracted from the measured thrust.

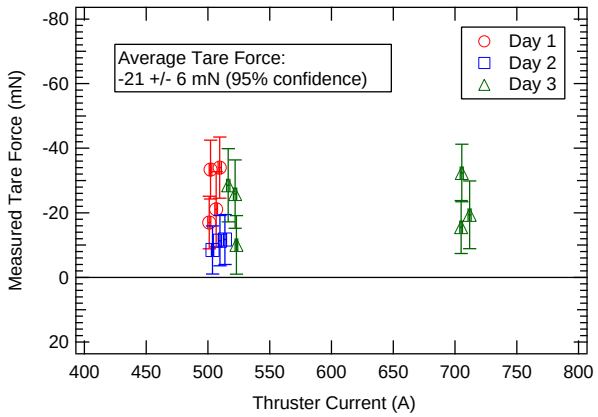

FIG. 14: The results of the tare force calibration of the PIPTS. This value is subtracted from the measured thrust to obtain the true thrust force.

VI. PIPST DEMONSTRATION WITH A LITHIUM-FED APPLIED-FIELD MPDT

The ability of the improved inverted pendulum thrust stand design (PIPTS) to accurately measure thrust was demonstrated during the firing of a 30-kW applied-field MPDT running on lithium propellant. Since the focus of this paper is on the thrust stand and thrust measurement technique, and not on the performance of MPD thrusters, we give only a representative measurement.

At a discharge current of 400 A, a nominal lithium flow rate of 17.5 mg/s, and an applied magnetic field strength of 0.1 T a typical thrust measurement was 274±27 mN. *In situ* calibrations of the stand immediately before and and after the thrust measurements showed consistent thrust stand behavior throughout the test and the sensitivity was determined to be 2.07 ± 0.07 mV/mN over the entire experimental run. Current induced forces were determined to be small (21 ± 6 mN) based on careful calibration prior to operating the thruster and were removed from the measured thrust to reduce the measurement error. The data was repeatable over several trials at the same operating conditions. The error is determined from the bias error associated with the sensitivity and tare force measurements and the precision error which is dominated by the error in determining the stand position before and after the thrust event.

VII. CONCLUSIONS

In this paper we have described the behavior of the inverted-pendulum method of thrust measurement for high-power plasma thrusters using an ideal analytical model and extensive calibrations. Two major sources of uncertainty in the thrust measurements were shown to exist: those due to changes in the sensitivity of the inverted pendulum on the time scale of the thrust measurement and those due to tare forces caused by thermal stresses and electromagnetic forces acting on the flexures. Our idealized analytical model showed that changes in sensitivity occur due to changes in the mass loading of the inverted pendulum and the temperature of the flexure elements. The sensitivity of the inverted pendulum can be increased only at the expense of more stringent requirements on the mass loading and thermal control. The results of the model are validated with measurements made using a carefully designed and calibrated inverted pendulum thrust stand. Several advantageous design features of the stand including gallium pots for current conduction, an optical two-axis displacement sensor, and careful consideration of flexure shape and cooling requirements. The sensitivity was demonstrated to be constant over a wide range of operating conditions. Measurements showed that thermal drifts of the stand were linear on the time scale of the thrust measurements and were less than 0.6% of the expected thrust (-1.5 ± 0.7 mN/C). The thrust stand operation was demonstrated during experiments with a 30-kW lithium-fed applied-field magnetoplasmadynamic

thruster and was shown to be repeatable and similar to behavior during calibrations. Under nominal conditions (500-600 A, 0.1 T, 17.5 mg/s). the thermal and electromagnetic tare forces were measured at less than 9% of the thrust and the thrust uncertainty at $\leq 10\%$ of the thrust (274$\pm$27 mN).

[1] J.E. Sovey and M.A. Mantenieks. Performance and lifetime assessment of magnetoplasmadynamic arc thruster technoloy. *Journal of Propulsion and Power*, 7:71–83, January 1991.

[2] G. Krülle, M. Auweter-Kurtz, and A. Sasoh. Technology and application aspects of applied field magnetoplasmadynamic propulsion. *Journal of Propulsion and Power*, 14:754–762, October 1998.

[3] A. D. Kodys and E. Y. Choueiri. A critical review of the state-of-the-art in the performance of applied-field magnetoplasmadynamic thrusters. In *41th AIAA/ASME/SAE/ASEE Joint Propulsion Conference*, number AIAA 2003-4247, Tucson, AZ, USA, 2005. , July 10-14.

[4] V. Kim, V. Tikhonov, and S. Semenikhin. Fourth quarterly (final) report to NASA-JPL: 100-150 kw lithium thruster research. Technical Report Contract NASW-4851, RIAME, MAI, Moscow, Russia, April 1997.

[5] T. W. Haag. Thrust stand for high power electric propulsion devices. *Rev. Sci. Instrum*, 5:1186–1191, May 1991.

[6] L. D. Cassady, A. D. Kodys, and E. Y. Choueiri. A thrust stand for high-power steady-state plasma thrusters. In *38th AIAA Joint Propulsion Conference*, number AIAA 2002-4118, Indianapolis, IN, USA, 2002. July 7-10.

[7] A. D. Kodys, L. D. Cassady, and E. Y. Choueiri. Thermal effects on inverted pendulum thrust stands for steady-state high-power plasma thrusters. In *39th AIAA Joint Propulsion Conference*, number AIAA 2003-4842, Huntsville, AL, USA, 2003. July 20-23.

[8] Andrea D. Kodys, Gregory Emsellem, Leonard D. Cassady, James E. Polk, and Edgar Y. Choueiri. Lithium mass flow control for high power Lorentz Force Accelerators. In *Space Technology and Applications International Forum*, number STAIF Paper 195, Albuquerque, New Mexico, USA, February 2001.

[9] D.W. Esker, J.C. Kroutil, and R.J. Checkley. Design and performance of radiation-cooled MPD arc thrustors. In *AIAA 7^{th} Electric Propulsion Conference*, number AIAA 69-245, Williamsburg, VA, USA, 1969. March 3-5.

[10] Denis J. Connolly, Ronald J. Sovie, Charles J. Michels, and James A. Burkhart. Low environmental pressure MPD arc tests. In *AIAA Electric Propulsion and Plasmadynamics Conference*, number AIAA- 67-685, Colorado Springs, CO, USA, 1967. September 11-13.

[11] Denis J. Connolly, Allan R. Bishop, and George R. Seikel. Tests of permanent magnet and superconducting magnet mpd thrusters. Number AIAA-1971-696, 1971. July.

[12] Thomas M. Golz, Monika Auweter-Kurtz, Harald Habiger, and Helmut L.. Kurtz. High specific impulse performance of a 100 kw radiation cooled thermal arcjet thruster. In *30^{th} AIAA/ASME/SAE/ASEE Joint Propulsion Conference*, number 94-3249, Indianapolis, IN, 1994. June 27-29.